between 16 kev and ~88 kev above this level. The experimental evidence on this point is not conclusive. Because of the limitations in equipment it was not possible to look for coincidences between the Pb M x-ray and the 987.8-kev gamma ray. This experiment should be done before any final conclusions are made.

Theoretical calculations by True,[16] using $\frac{3}{4}$ singlet-even forces plus weak coupling, indicate that a $13/2^+$ level would be expected at approximately 1050 kev. These calculations also predict a $7/2^-$ level at 930 kev and a $9/2^-$ level at 940 kev. These are interpreted by True as the 987.8-kev and the 1002.7- or 1014.2-kev levels, respectively, in Pb²⁰⁵. If the $9/2^-$ level were interpreted as the 987.8-kev level and the $7/2^-$ level were interpreted as either the 1002.7- or 1014.2-kev level then it would be possible for the $13/2^+$ level at approximately 1050 kev to feed the $9/2^-$ level at 987.8 kev. If this were the case, the 1050-kev level would decay by an $M2$ transition. For an $M2$ transition of 60 kev, the expected half-life is 220 msec.[14] Although this is not in good agreement with the measured value of the 4.8

---

[16] W. W. True (private communication).

msec the disagreement is not so severe as to eliminate this possibility. Because of experimental limitations this low-energy gamma ray was not seen. A search for it should be made using more sensitive techniques.

ACKNOWLEDGMENTS

The authors wish to acknowledge the help of E. C. Yates, D. G. Proctor, E. H. Turk, R. P. Schuman, G. O. English, and W. Hammer in performing the experimental work. Discussions with W. W. True and G. Andersson proved to be both stimulating and enlightening.

Note added in proof.—Electron conversion lines in the decay of Bi²⁰⁵ corresponding to a transition energy of approximately 26 kev have been observed by D. E. Alburger (private communication). R. Stockendal (private communication) has also observed electron conversion lines corresponding to a transition energy of 26.2 kev. Electron-gamma coincidence measurements by Alburger have confirmed that this transition is in coincidence with a strong gamma ray of 1 Mev (presumably the 987.8-kev gamma ray). This evidence, together with that presented in this paper, has led to the conclusion that the 987.8-kev level is not isomeric but rather is fed entirely by the 26.2-kev transition. This implies that the isomeric level is at 987.8+26.2=1014.0 kev.

Interaction of K^+ Mesons with Protons*

T. F. KYCIA,† L. T. KERTH, AND R. G. BAENDER
Lawrence Radiation Laboratory, University of California, Berkeley, California
(Received September 11, 1959)

The total K^+-p cross section was measured at the three K^+-meson energies 175±25, 225±25, and 275±25 Mev, and the differential scattering cross section was measured at 225 Mev. The K^+-p nuclear force was shown to be repulsive, from the observed constructive interference with Coulomb scattering. The differential cross section was otherwise isotropic and could arise from either pure S-wave or pure P-wave scattering.

Subtracted dispersion relations were applied to these data and the rest of the available K-proton scattering data. The statistical errors in the data were found to be too large to determine the K-hyperon relative parity. On the assumption that the $K\Lambda$ and $K\Sigma$ relative parities are the same, then for scalar coupling, $g^2/4\pi$ would be less than 0.6; for pseudoscalar coupling, it would be less than 10.

I. INTRODUCTION

INFORMATION on the scattering of K^+ mesons on protons is of the greatest importance, in that it may allow us to determine the nature of the K-meson-nucleon forces. Data at low energies have come mostly from the rare scattering of K^+ mesons on hydrogen nuclei in emulsion. A compilation of the world total of 75 events was reported at the 1958 High-Energy Physics Conference at CERN.[1] The angular distributions in the three

---

* Work done under the auspices of the U. S. Atomic Energy Commission.

† Present address: Brookhaven National Laboratory, Upton, New York.

[1] M. F. Kaplon, *1958 Annual International Conference on High-Energy Physics at CERN*, edited by B. Ferretti (CERN Scientific Information Service, Geneva, 1958).

energy intervals 20 to 100 Mev, 100 to 200 Mev, and 200 to 300 Mev, considering the large uncertainties, were not inconsistent with isotropy.

From a more recent compilation of data,[2] total cross sections have been obtained as shown in Table I.

TABLE I. Results from experiments with nuclear emulsions.

Energy (Mev)	Total K^+-p cross sections (mb)
20–100	13.5±2.8
100–200	14.2±2.6
200–300	18.0±3.5

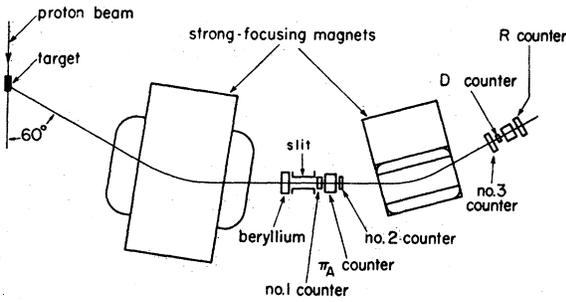[2] D. H. Stork and D. J. Prowse, University of California (private communication).

FIG. 1. Beam arrangement. K^+ mesons were produced in a tantalum target and, after the elimination of proton contamination by means of a beryllium absorber, were focused on Counter D.

The purpose of this experiment was to measure the total K^+-meson-proton cross section at the higher energies—namely, 175 ± 25, 225 ± 25, and 275 ± 25 Mev—as well as to determine the differential scattering cross section with small statistical errors at 225 Mev. If the rise in total cross section should be due to a rising P-wave contribution, an asymmetry in the differential scattering cross section should be detected.

II. K^+-MESON SELECTION

A. The K^+-Meson Beam

The scattering-detection system required that the K^+ beam should be (a) of angular divergence less than $\pm2°$ at the entrance to the liquid hydrogen target, (b) focused in an area of 1.25-in. diameter, (c) of energy spread no greater than ±25 Mev, (d) of an intensity

greater than 25 K^+ mesons per bevatron pulse. These requirements were met for beam energies of 175 ± 25, 225 ± 25, and 275 ± 25 Mev, with the arrangement illustrated in Fig. 1.

The K^+ mesons were produced in a tantalum target located in a bevatron straight section, and entered the first of two 4-in.-aperture double-lens strong-focusing bending magnets. The first magnet momentum-analyzed the incoming particles, and focused the particles with the desired momentum at the lead slit. The beryllium was necessary to reduce the proton contamination. The second magnet refocused the selected particles at the D-scintillation counter.

B. K^+-Meson Identification

The portion of the beam that passes through the lead slit consists of K^+ and π^+ mesons and protons, but the particles focused at Counter D consist mainly of K^+ and π^+ mesons. The proton contamination at this point is negligible. The K^+ mesons are distinguished from the π^+ mesons by time of flight over the 8 feet between Counters 1 and D.

To attain a high time resolution for the identification system, the K^+ mesons were identified by requiring a coincidence of scintillation counters 1, 2, 3, D and anticoincidence with π_A, a velocity-threshold Čerenkov counter which was used to identify π^+. The π^+ contamination in the identified K^+ beam was measured to be less than 0.7%. A block diagram of the circuitry is shown in Fig. 2.
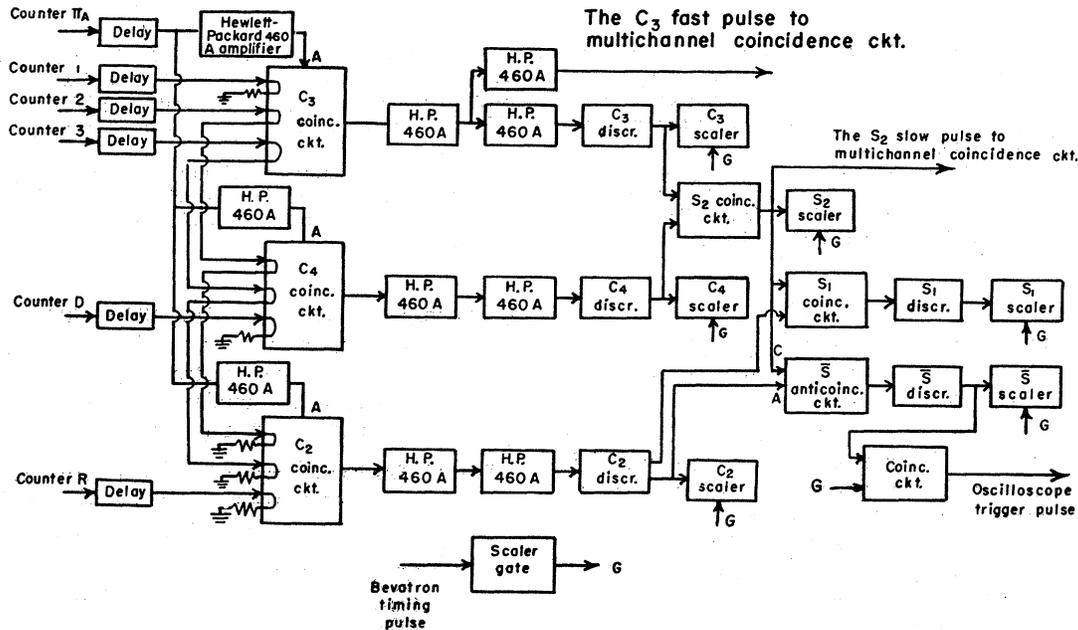

FIG. 2. Block diagram of K^+-meson identification circuiting. Coincidences and anticoincidences were taken between counters 1, 2, 3, D, and π_A, and scaled. The S_2 scaler then indicated the number of K^+ mesons that entered the target; the S_1 scaler indicated the number of K^+ mesons that passed through the target; the $\bar{S}$ scaler indicated the number of K^+ mesons that disappeared from the beam between Counters D and R. This $\bar{S}$ anticoincidence-circuit pulse triggered an oscilloscope, upon which were displayed the ring-counter pulses.

The R counter of Fig. 1 was used for range-energy measurements. By inserting copper between Counters D and R, we could determine the range distribution in copper, and thus the energy distribution of the K^+ mesons. Suitable corrections for K^+ decays between counters D and R were applied.

III. SCATTERING-DETECTION SYSTEM

Figure 3 shows the scattering angles of the K^+ meson and the proton in the laboratory system as a function of the angle in the center-of-mass of the K^+ meson, for elastic K^+-p scattering. The kinematics are insensitive to incident K^+ energies in the range 175–275 Mev. It is seen that one and only one of the two particles enters a forward cone of half-angle 50° (lab). Thus, to determine the angular distribution of the scattered K^+ mesons, it was sufficient to determine the angle of the forward-scattered particle and then to identify the particle as
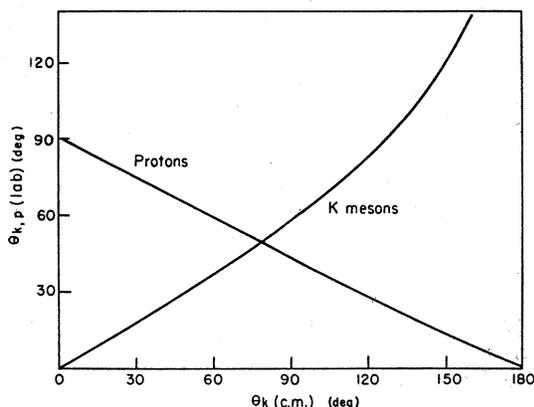
FIG. 3. The laboratory system scattering angle of protons and K^+ mesons, as a function of the center-of-mass system scattering angle of the K^+ meson, for a K^+-p elastic scattering event.

being either a K^+ meson or a proton. The inelastic K^+-p scattering giving rise to π-meson production is assumed to be small.[3]

After the energy of the K^+ beam was determined with the arrangement illustrated in Fig. 1, the R counter was removed and the arrangement illustrated in Fig. 4 was placed behind the D counter. The T counter of Fig. 4 replaced the R counter of Fig. 1 in the circuitry of Fig. 2.

The liquid hydrogen was contained in a thin-walled Mylar vessel 6 in. in length and 3 in. in diameter. A double bank of ring counters was used to determine the angle of the scattered particles. Each ring counter overlapped the adjacent one, to improve the angular definition. To define the scattering angle, it was necessary for at least one counter from each bank to count. With this arrangement, the scattering angle could be defined to within ±5° (lab).

The ring counter pulses, together with the R pulse

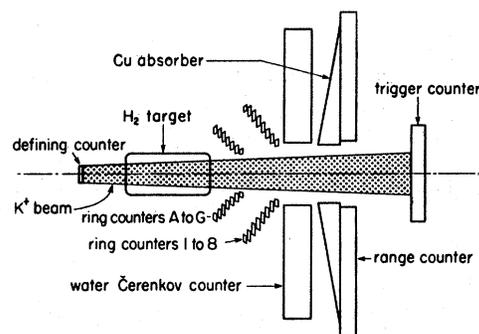[3] E. Helmy, J. H. Mulvey, D. J. Prowse, and D. H. Stork, Phys. Rev. 112, 1793 (1958).

FIG. 4. Arrangement of liquid hydrogen target and scattering-detection scintillation counters. The line of flight of the scattered particle is determined by the double bank of ring counters, and the particle is identified by its range in copper.

from counter R of Fig. 4, the C pulse from the water Čerenkov counter of Fig. 4, the T pulse from the trigger counter of Fig. 4, and a timing pulse were displayed on an oscilloscope with the aid of the circuitry of Figs. 3 and 5, and the traces were photographed.

The water Čerenkov counter shown in Fig. 4 was used to identify the decay products originating from the large number of K^+ decays in the region behind the defining counter. Approximately 98% of the decay products originating from the six different K^+-meson decay modes had velocities great enough to excite the Čerenkov counter. For the most part, the C pulse from the water Čerenkov counter was used to blank the oscilloscope. The oscilloscope was allowed to record events in which the C pulse appeared only for that part of the experiment in which the ring counters were calibrated on the decay products.

The copper absorber and range counter, located behind the water Čerenkov counter in Fig. 4 were used to identify the scattered particle. The copper was just thick enough to stop the protons for all lab angles between 12° and 50°, while the K^+ mesons passed through the copper and registered in the range counter.

IV. THE TOTAL K^+-p CROSS SECTION

The total K^+-p cross sections at the three energies of 175±25, 225±25, and 275±25 Mev were obtained from the $\bar{S}$- and S_2-scaler readings. The S_2 readings gave the number of K^+ mesons passing through the defining counter, whereas the $\bar{S}$ reading gave the number of K^+ mesons that passed through the defining counter but did not reach the T counter. The $\bar{S}$ and S_2 readings were accumulated for "target full" and "target empty," for each of the three energies. Table II lists these numbers as well as the ratios of $\bar{S}/S_2$, which are the fractions of K^+ mesons removed from the K^+ beam.

From the target-empty data in Table II, one sees that the background from decays, scattering in the walls of the target, and scattering in the defining counter is approximately 10 to 15 times as large as the effect under investigation. The total cross section was obtained from
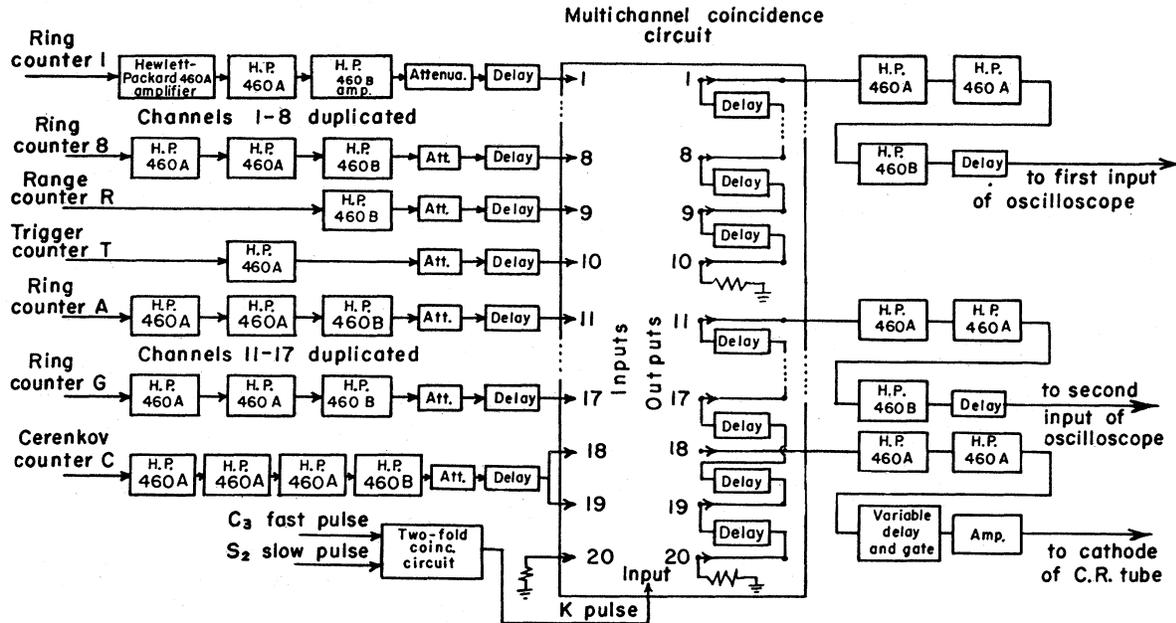
FIG. 5. Block diagram of scattering-detection circuitry. In the multichannel coincidence circuit, the scattering-detection scintillation-counter pulses are put into coincidence with an S_2-coincidence-circuit pulse and then displayed on an oscilloscope.

the difference of the two relatively large quantities $\bar{S}/S_2|f$ and $\bar{S}/S_2|e$ by means of Eq. (1), which takes into account as well as possible the difference in decay rates for "target full" and "target empty" conditions. The background from wall scattering, etc. was small in comparison with the decay background, and was presumed to be the same for both "target full" and "target empty" conditions. In addition, the "target empty" condition actually included scatterings from the hydrogen gas still in the "empty" target. The gas density at that temperature is approximately 2% of the liquid density.

Assuming all decays and scattering events to take place on the beam axis, and neglecting multiple scatters, we have

$$\frac{N(x_1)}{N(x_0)} = \exp\left\{ - \int_{x_0}^{x_1} [\lambda_s(x) + \lambda_D(x)]dx \right\}, \quad (1)$$

where $N(x_1)$ is the number of K^+ mesons in the beam at point x_1; $N(x_0)$ is the number of K^+ mesons in the beam at point x_0; $\lambda_s(x) = n(x)\sigma(x)$; $n(x) =$ target nuclei den-

TABLE II. Summary of scaler readings.

Scaler	Energy (Mev)		
	175±25	225±25	275±25
$\bar{S}|f$ (target full)	68 195	105 646	34 684
$S_2|f$	415 582	742 672	275 308
$\bar{S}|e$ (target empty)	68 063	44 944	30 014
$S_2|e$	442 917	338 033	258 375
$(\bar{S}/S_2)|f$	0.1641	0.1423	0.1260
$(\bar{S}/S_2)|e$	0.1537	0.1330	0.1162

sity, and $\sigma(x)$ is the cross section for scattering into angles great enough to miss the T counter; $\lambda_D(x)$ is the reciprocal decay length for decays in which the charged decay product misses the T counter; x_1 is taken at the T counter, so that $N(x_1) = S_2 - \bar{S}$, where S_2 and $\bar{S}$ are scaler readings. x_0 is taken immediately before the D counter, so that $N(x_0) = S_2$.

The integrals

$$\int_{x_0}^{x_1} [\lambda_s(x) + \lambda_D(x)]dx$$

were performed for "target full" and "target empty"; $\bar{S}/S_2$-scaler data were substituted into the left side of Eq. (1), and then Eq. (1) was solved for the $K^+ - p$ cross section for scattering into angles $>12°$. The results of the calculations are given in Table III. The experimental error in the K^+-meson half life led to a calculated error of $<1\%$ in the total cross section, and was neglected.

V. THE K^+-p DIFFERENTIAL CROSS SECTION

A. Calculation of the Differential Cross Section

For the total cross-section determination, it was a good approximation to consider all events to occur on the target axis, for the derivation of Eq. (1). The added complexity of the geometry due to the introduction of the ring counters into the system, coupled with the desire to get a fairly accurate measure of the differential cross section, necessitated taking into account the off-axis events.

To this purpose, let: $\bar{r} =$ the position vector of an

arbitrary point within the target, $d\tau$ = a volume element of target, θ = the scattering angle of a scattering event, $P_S(\theta,\bar{r})d\theta d\tau$ = the probability that a scattering event occurs in the volume element $d\tau$ at $\bar{r}$ and scatters into the angular interval $d\theta$ at θ, $P_c(\theta,\bar{r})$ = the probability that the ring counter combination c will receive a scattered particle, computed on the information that the particle scattered in the volume element $d\tau$ at $\bar{r}$ into the angular interval $d\theta$ at θ, ϵ = the counting efficiency of counter combination c (assumed to be a constant), $\bar{S}_c$ = the experimental number of events detected by counter combination c as ascertained from the film data. Then $\bar{S}_c/S_2|_{\text{full}}$ is the fraction of the incident K^+ mesons that scattered into counter combination c. We may then write

$$\bar{S}_c/S_2|_{\text{full}} - \bar{S}_c/S_2|_{\text{empty}}$$
$$= \int_{\theta_1}^{\theta_2}\left[\int_R \epsilon P_S(\theta,\bar{r})P_c(\theta,\bar{r})d\tau\right]d\theta, \quad (2)$$

where θ_1, θ_2 are the limiting angles at which counter combination c can detect a scattering event that occurred within the region R, and R is the region of the target accessible to the incident K^+-meson beam. Of course the integration indicated in Eq. (2) would be impossible to carry out directly. However, some simplification is possible. We may approximate $P_S(\theta,\bar{r})$ by

$$P_S(\theta,\bar{r}) = nd\sigma/d\theta|_L, \quad (3)$$

where n = number of target protons per unit volume (assumed to be constant) and $d\sigma/d\theta|_L$ is the differential scattering cross section in the laboratory system. The effect of the decrease in K^+ flux through the target, which renders Eq. (3) only an approximation, is treated as a correction to be applied later. We then have, from Eq. (2),

$$\bar{S}_c/S_2|_{\text{full}} - \bar{S}_c/S_2|_{\text{empty}}$$
$$= n\epsilon\langle d\sigma/d\theta|_L\rangle\int_{\theta_1}^{\theta_2}\int_R P_c(\theta,\bar{r})d\tau d\theta$$
$$= n\epsilon\langle d\sigma/d\theta|_L\rangle\int_{\theta_1}^{\theta_2} P_c'(\theta)d\theta, \quad (4)$$

where

$$\langle d\sigma/d\theta|_L\rangle = \int_{\theta_1}^{\theta_2}\int_R d\sigma/d\theta|_L P_c(\theta,\bar{r})d\tau d\theta$$
$$\div \int_{\theta_1}^{\theta_2}\int_R P_c(\theta,\bar{r})d\tau d\theta, \quad (5a)$$

TABLE III. Corrected total $K^+ - p$ cross sections from scaler data.

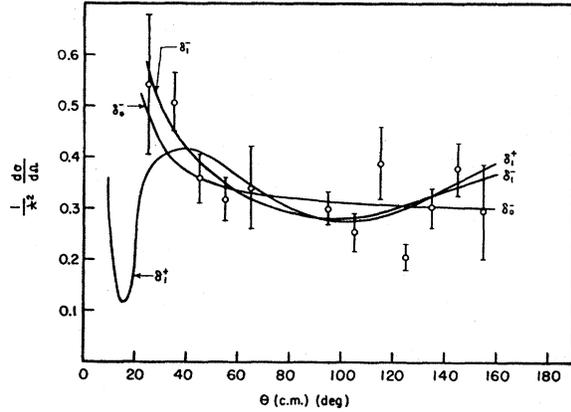| Energy (Mev)	Total $K^+ - p$ cross section (mb)
175±25	16.3±1.7
225±25	15.2±1.3
275±25	16.3±1.7

FIG. 6. The $K^+ - p$ differential scattering cross section at 225 ±25 Mev, in units of the square of the center-of-mass system de Broglie wavelength of the K^+ meson. The curves labeled $\delta_0{}^-$, $\delta_1{}^-$, and $\delta_1{}^+$ are least-square fits for, respectively, $S_{\frac{1}{2}}$-state scattering with repulsive nuclear potential, $P_{\frac{1}{2}}$-state scattering with repulsive nuclear potential, and $P_{\frac{3}{2}}$-state scattering with attractive nuclear potential.

and

$$P_c'(\theta) = \int_R P_c(\theta,\bar{r})d\tau. \quad (5b)$$

The integration indicated in Eq. (5b) was carried out by means of the Monte Carlo method, using an IBM 701 computer, and the $P_c'(\theta)$ were thus obtained. For each θ (in 1-deg intervals) 1000 scattering events were simulated by the computer at random positions inside the hydrogen target and at random azimuthal angles. The efficiency factor ϵ for each counter combination was determined by comparing the observed counts from K-meson decays with theoretical values. The counts from decays were obtained by turning off the Čerenkov blanking pulse to the oscilloscope. The theoretical values were calculated on the basis of isotropic decay in the center-of-mass system for each decay mode.

From the definition of $P_c'(\theta)$ [Eq. (5b)] and from the definition of the angles θ_1 and θ_2 [Eq. (2)], it follows that $P_c'(\theta) \equiv 0$ for $\theta \leqslant \theta_1$ and for $\theta \geqslant \theta_2$. Thus θ_1 and θ_2 could be determined by graphing $P_c'(\theta)$. It was found, for each counter combination considered, that $P_c'(\theta)$ was fairly symmetric about $(\theta_1+\theta_2)/2$. Thus, since $d\sigma/d\theta|_L$ is independent of $\bar{r}$ and is assumed to be a slowly varying function of θ, we have from Eq. (5a),

$$\langle d\sigma/d\theta|_L\rangle \approx d\sigma/d\theta|_L(\theta_1+\theta_2)/2, \quad (6)$$

where the right side of this last expression is to be interpreted as $d\sigma/d\theta_L$ considered as a function of θ_{lab} and evaluated at $(\theta_1+\theta_2)/2$.

More than 100 counter combinations were used to obtain the differential cross section. To improve the statistics and make the approximation of Eq. (6) more accurate, counter combinations were grouped together

so that their combined counts indicated scatters into $\pm 10°$ about θ(c.m.).

B. Corrections

Correction factors were applied, taking into account: (a) decays of the scattered mesons, (b) scattered K^+ mesons that interact in the Cu absorber, and (c) decrease in K flux along the axis of the target. These corrections were a function of angle, and amounted to about 10%. The corrected results of the calculations based on Eqs. (4) and (6) and the transformation to center-of-mass coordinates are given in Fig. 6, where $d\sigma/d\Omega = (2\pi \sin\theta)^{-1}d\sigma/d\theta|_{\text{c.m.}}$.

From the phase-shift analysis described in the next section, using the $S_{\frac{1}{2}}$ $K^+ - p$ scattering-state phase shift obtained from the data of Fig. 6, the total $K^+ - p$ scattering cross section was calculated as $\sigma_T = 15.3$, in good agreement with the value 15.2 ± 1.3 mb obtained from the scaler data.

VI. PHASE-SHIFT ANALYSIS

The angular distribution of the scattering of K^+ mesons from protons has been analyzed in terms of an expansion in partial waves. We assumed that since $\lambda \approx 0.6 \times 10^{-13}$ cm, the compound K^+-meson nucleon states responsible for the scattering were $s_{\frac{1}{2}}$, $p_{\frac{1}{2}}$, $p_{\frac{3}{2}}$. From the assumption of charge independence for the nuclear interaction between the K meson and nucleon, it follows the K^+ mesons are scattered from protons in a pure $T = 1$ isotopic spin state. The number of phase shifts necessary to describe the differential cross section was thus reduced to three, namely, δ_0, and δ_1, and δ_3 for scattering in the $s_{\frac{1}{2}}$, $p_{\frac{1}{2}}$, and $p_{\frac{3}{2}}$ states, respectively. It is possible to determine experimentally the absolute signs of the phase shifts from the interference of the nuclear scattering with the Coulomb scattering.

The differential cross section in the center-of-mass system for scattering without and with spin flip and including the Coulomb effect is[4]

$$\frac{d\sigma}{d\Omega}\bigg|_{nf} = \frac{\lambda^2}{4}\left|\frac{-\alpha}{\sin^2(\theta/2)}\exp[-i\alpha \ln \sin^2(\theta/2)] + P + Q \cos\theta\right|^2, \tag{7}$$

$$\frac{d\sigma}{d\Omega}\bigg|_{f} = \frac{\lambda^2}{4}|R|^2 \sin^2\theta, \tag{8}$$

where: λ is the de Broglie wavelength of the K^+ meson in the center-of-mass system,

$$\alpha = \mu e^2 \lambda / \hbar^2 (1 - \beta^2)^{\frac{1}{2}};$$

μ, e, $\hbar$ are the reduced mass of the K^+-meson proton system, the K^+-meson charge, and Planck's constant, respectively; β is the velocity of the K^+ meson relative to the proton;

$$P = e^{2i\delta_0} - 1,$$

$$Q = 2i\left(\frac{1+i\alpha}{1-i\alpha}(\sin\delta_1 e^{i\delta_1} + 2 \sin\delta_3 e^{i\delta_3})\right),$$

$$R = 2i(\sin\delta_3 e^{i\delta_3} - \sin\delta_1 e^{i\delta_1}).$$

Some simplification is possible. For a K^+-meson energy of 225 Mev, $\alpha = 0.014$. Thus, α can be neglected in Q without contributing more than 3% uncertainty in the scattering amplitude. The expression $\exp[-i\alpha \ln \sin^2(\theta/2)]$ can be set equal to unity for $\theta > 20°$, for $\alpha \ln \sin^2(\theta/2) < 0.02$.

The combination of the differential cross sections for scattering without and with spin flip, in units of λ^2, is

$$(1/\lambda^2)d\sigma(\mu)/d\Omega$$
$$= \{|[-\alpha/(1-\mu)] + \sin\delta_0 e^{i\delta_0} + (\sin\delta_1 e^{i\delta_1} + 2 \sin\delta_3 e^{i\delta_3})\mu|^2$$
$$+ |\sin\delta_3 e^{i\delta_3} - \sin\delta_1 e^{i\delta_1}|^2(1-\mu^2)\}, \tag{9}$$

where $\mu = \cos\theta$.

A good fit of $(1/\lambda^2)[d\sigma(\mu)/d\Omega]$ to the experimentally determined differential cross sections corresponds to a minimum in

$$\chi^2 = \sum_i \left(\frac{y(\mu_i) - (1/\lambda^2)[d\sigma(\mu_i)/d\Omega]}{\sigma(\mu_i)}\right)^2, \tag{10}$$

where $y(\mu_i)$ and $\sigma(\mu_i)$ are the experimental cross sections and their statistical errors, respectively. The IBM 650 computer was programmed to calculate χ^2 from Eqs. (9) and (10) for a set of arbitrary values of the three phase shifts, δ_0, δ_1, δ_3. One of the phase shifts was then increased by 0.01 radian, and the χ^2 recalculated. If the new χ^2 was smaller than the previous one, the phase shift was changed again in the same direction. If χ^2 was larger, the phase shift was then decreased. The process was repeated until χ^2 reached a minimum, and then another phase shift was varied. When χ^2 could not be made smaller by changing any of the three phase shifts, the coputerm gave the result. By starting with various sets of initial phase shifts, three solutions were found that gave a χ^2 small enough to be considered significant. These are given in Table IV. The χ^2 for each solution, as well as the confidence level, is listed. The fit with $\delta_0 > 0$ and $\delta_1 = \delta_3 \approx 0$ gave a confidence of less than 1%. The δ_0^- and δ_1^- solutions correspond to interactions in virtually pure $s_{\frac{1}{2}}$ and $p_{\frac{1}{2}}$ states, respectively, with phase shifts of approximately $-33°$. Both solutions also agree with the forward peaking in the cross section, indicating a repulsive nuclear potential. For the δ_1^+ solution, the rise in the determined measured cross section at 25° and

[4] L. Van Hove, Phys. Rev. 88, 1358 (1952).

35° does not agree with the predicted drop. The ambiguity between δ_0^- and δ_1^- is considered in greater detail in the following section.

VII. DISCUSSION

A. Total Cross Section

Knowledge of the K^+-meson-proton interaction has been extended to intermediate kinetic energies. Our results in Table III confirm the increase in K^+-meson-proton cross section as a function of energy found from the scattering of K^+ mesons on free protons in nuclear emulsion.[1] Our averaged cross section over the energy interval from 200 to 300 Mev is 15.6 ± 1.0 mb, which agrees within the statistical errors with 18.0 ± 3.5 mb obtained from emulsion events (for comparison, the cross section below 100 Mev is 13.5 ± 2.5 mb).[2] The threshold for π-meson production by K^+ mesons on protons is 225 Mev. Our total cross sections include the contribution from π-meson production, but no estimate of the magnitude could be made.

Recent data from 600 Mev to 2 Bev indicate that the total cross section rises to 19.6 ± 1.2 mb at 700 Mev and then gradually drops to 13.0 ± 1.0 mb at 2 Bev.[5] The over-all behavior of the K^+-meson proton cross section as a function of energy is not understood at present.

B. The Nature of the K^+-Meson Force

Of the three phase-shift combinations that were found to fit the angular distribution of the scattered K^+ mesons, only two (namely, δ_0^- and δ_1^-) gave good agreement with the small-angle scattering. If we consider only the data less than 40 deg where there is a significant difference between the three calculated curves, we find a significance level of $\sim20\%$ for δ_1 and for δ_0^-, while it is less than 1% for δ_1^+. Although both solutions are about equally probable, it is important to note that both correspond to a repulsive K^+-meson proton force. This evidence in favor of the repulsive nuclear force is indeed the most direct and conclusive yet obtained. Supporting evidence has come in the past from the optical-model analyses of inelastic scattering of K^+ mesons from emulsion nuclei.[1]

TABLE IV. Phase-shift combinations that give good agreement with experimental data.

Solution	δ_0 (deg)	δ_1 (deg)	δ_3 (deg)	x^2	Confidence level (%)
δ_0^-	-33.4 ± 2.3	-0.7 ± 5.7	-0.1 ± 3.4	10.6	21
δ_1^-	-0.6 ± 3.2	-34.2 ± 2.3	-2.2 ± 2.5	6.5	59
δ_1^+	4.3 ± 2.7	35.4 ± 2.9	3.7 ± 1.8	11.9	17

[5] H. C. Burrowes, D. O. Caldwell, D. H. Frisch, D. A. Hill, D. M. Ritson, and R. A. Schluter, Phys. Rev. Letters **2**, 117 (1959).

C. The Differential Scattering Cross Section

The δ_0^-, δ_1^- ambiguity in the phase shifts to the experimental data cannot be easily resolved. For the δ_1^- solution, one would expect the recoil proton to be polarized. However, since the polarization arises from the interference with the Coulomb scattering, the predicted value has a maximum of $P(\theta)=0.07$ for $\theta=70°$ (lab). It may be easier to resolve the ambiguity by measuring the differential cross section of K^+ mesons scattering from protons at lower energies. If the differential cross section is isotropic for all energies, and if one assumes that K^+ mesons scatter in the S wave at very low energies, then the δ_0^--phase-shift combination must be the true solution. This follows from the fact that to change from pure S-wave scattering to pure $P_{\frac{1}{2}}$-wave scattering, the cross section must be anisotropic in the energy interval in which both S and P waves contribute to the scattering cross section.

D. Use of K^+-p Dispersion Relations

The form of the $K-p$ dispersion relations is[6]

$$D_{\pm}(\omega)=\frac{1}{4\pi^2}\int_1^\infty \frac{k'\sigma_+(\omega')}{\omega'\mp\omega}d\omega'+\frac{1}{4\pi^2}\int_1^\infty \frac{k'\sigma_-(\omega')}{\omega'\pm\omega}d\omega'$$

$$+\frac{1}{4\pi^2}\int_{\omega_{\Lambda\pi}}^1 \frac{4\pi A_-(\omega')}{\omega'\pm\omega}d\omega'$$

$$+\frac{p_\Lambda X(\Lambda)}{\omega_\Lambda\pm\omega}+\frac{p_\Sigma X(\Sigma)}{\omega_\Sigma\pm\omega}+C, \quad (11)$$

where $D_\pm$ is the real part of the K^+-proton forward-scattering amplitude, in units of K-meson Compton wavelength (λ_c); k' is the laboratory-system momentum, in units of $m_k c$; ω' and ω are laboratory-system energies of the K meson, in units of $m_k c^2$; $\sigma_+(\omega')$ and $\sigma_-(\omega')$ are the K^+-p and K^--p total cross sections, respectively, in units of K-meson Compton wavelength, squared; A_- is the imaginary part of the K^--p forward-scattering amplitude, in units of K-meson Compton wavelength; C is a constant.

The purpose of this section is to investigate the possibility of determining $p_\Lambda(p_\Sigma)$ and $X(\Lambda)[X(\Sigma)]$, which are the sign and magnitude of the residues at $\omega=m_\Lambda(m_\Sigma)$, respectively, where

$$X_{\Lambda,\Sigma}=\frac{g_{\Lambda,\Sigma}^2}{4\pi}\left[\frac{\pm(m_{\Lambda,\Sigma}\pm m_p)^2\mp m_k^2}{4m_p m_{\Lambda,\Sigma}}\right], \quad \text{for } p_{\Lambda,\Sigma}=\pm1. \quad (12)$$

The quantities p_Λ and p_Σ are either $+1$ or -1,

[6] There is much literature on the subject, but a few pertinent references are: D. Amati and B. Vitale, Nuovo cimento **7**, 190 (1958); K. Igi, Progr. Theoret. Phys. (Kyoto) **3**, 238 (1958); C. Goebel, Phys. Rev. **110**, 572 (1958); P. T. Matthews and A. Salam, Phys. Rev. **110**, 565, 569 (1958).

depending upon the parity of the K-hyperon nucleon system. We have

$$\omega_\alpha = \frac{m_\alpha{}^2 - m_p{}^2 - m_k{}^2}{2m_p}, \qquad (13)$$

where m_α is the rest energy of the α system ($\omega_\Lambda = 0.129 m_k$, $\omega_\Sigma = 0.313 m_k$, and $\omega_{\Lambda\pi} = 0.498 m_k$).

Of the various subtracted dispersion relations proposed, none is adequate at present for the experimental data now available. The following form, however, has several decisive advantages.

$$\omega_0 D_+(\omega) - \tfrac{1}{2}(\omega_0 + \omega)D_+(\omega_0) - \tfrac{1}{2}(\omega_0 - \omega)D_-(\omega_0)$$

$$= \frac{1}{4\pi^2}\int_1^\infty \left(\frac{\omega_0 k'\sigma_+(\omega')}{\omega' - \omega} - \frac{(\omega_0 + \omega)k'\sigma_+(\omega')}{2(\omega' - \omega_0)} - \frac{(\omega_0 - \omega)k'\sigma_+(\omega')}{2(\omega' + \omega_0)}\right)d\omega'$$

$$+ \frac{1}{4\pi^2}\int_1^\infty \left(\frac{\omega_0 k'\sigma_-(\omega')}{\omega' + \omega} - \frac{(\omega_0 + \omega)k'\sigma_-(\omega')}{2(\omega' + \omega_0)} - \frac{(\omega_0 - \omega)k'\sigma_-(\omega')}{2(\omega' - \omega_0)}\right)d\omega'$$

$$+ \frac{1}{4\pi^2}\int_{\omega_{\Lambda\pi}}^1 \left(\frac{\omega_0 4\pi A_-(\omega')}{\omega' + \omega} - \frac{(\omega_0 + \omega)4\pi A_-(\omega')}{2(\omega' + \omega_0)} - \frac{(\omega_0 - \omega)4\pi A_-(\omega')}{2(\omega' - \omega_0)}\right)d\omega'$$

$$+ p_\Lambda X(\Lambda)\left(\frac{\omega_0}{\omega_\Lambda + \omega} - \frac{\omega_0 + \omega}{2(\omega_\Lambda + \omega)} - \frac{\omega_0 - \omega}{2(\omega_\Lambda - \omega)}\right) + p_\Sigma X(\Sigma)\left(\frac{\omega_0}{\omega_\Sigma + \omega} - \frac{\omega_0 + \omega}{2(\omega_\Sigma + \omega)} - \frac{\omega_0 - \omega}{2(\omega_\Sigma - \omega)}\right). \qquad (14)$$

If ω_0 is set equal to m_k in (14), Igi's form is obtained.[7] The above form, however, has the advantages of Igi's in that the cross-section integrals converge rapidly and depend more on the $K^+ - p$ cross sections than on those of $K^- - p$. These cross-section integrals converge, even if the cross sections go to a constant as ω goes to infinity. An additional advantage of form (14) is that the real parts of the forward-scattering amplitudes are used at energies for which they are known from experiment, rather than at the rest energy. Furthermore, the contribution from the unphysical region is decreased by displacing a singularity from its position at m_k to ω_0.

The latest experimental $K - p$ total cross sections were used for $k\sigma_\pm(\omega)$.[2,5,8–10] A smooth curve was fitted to the experimental points, and an extrapolation of $4\pi A_-$ was made into the unphysical region. More precise estimates on the extrapolation into the unphysical region have been carried out by Dalitz and Tuan.[11] Their values do not materially affect the conclusions from the dispersion relations.[12] Since the dispersion relation in Eq. (14) does not weight the high-energy region, it was possible to make cutoffs at $\omega = \pm 4$. The statistical errors were estimated to be 10% for the integral under the smooth curve fitted to $k\sigma_+(\omega)$, and 15% for $k\sigma_-(\omega)$. Figure 7 shows a typical integrand for the integral of

Eq. (14). The experimental points are shown, to indicate the effect of the experimental uncertainties.

The quantity $D_\pm(\omega)$ was obtained from

$$D_\pm(\omega) = \pm \frac{\omega}{m_p}\left(\frac{d\sigma_\pm{}^{el}}{d\Omega}(\omega)\Big|_{\theta=0} - \frac{k_b{}^2}{16\pi^2}[\sigma_\pm(\omega)]^2\right)^{\frac{1}{2}}, \qquad (15)$$

where ω and k_b are, respectively, the total energy and K-meson momentum in the center-of-mass frame. The sign of $D_\pm(\omega)$ is plus or minus, depending upon whether the K^+-proton force is attractive or repulsive, respectively. From the experiment being described, it has been seen that the $K^+ - p$ interaction is repulsive, thus making $D_+(\omega)$ negative. The nature of the $K^- - p$ force is still unknown, and this causes $D_-(\omega)$ to be uncertain in sign.
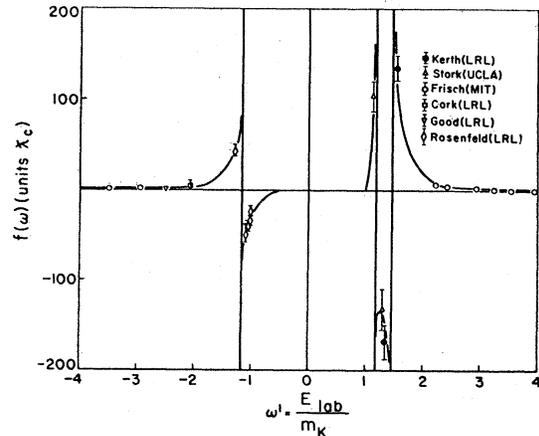
[7] K. Igi, Progr. Theoret. Phys. (Kyoto) 4, 403 (1958).

[8] B. Cork, G. R. Lambertson, O. Piccioni, and W. Wentzel, Phys. Rev. 106, 167 (1957).

[9] L. W. Alvarez, P. Eberhard, M. L. Good, W. Graziano, H. K. Ticho, and S. G. Wojcicki, Lawrence Radiation Laboratory (private communication).

[10] P. Nordin, A. H. Rosenfeld, F. T. Solmitz, R. D. Tripp, and M. B. Watson, Bull. Am. Phys. Soc. 4, 288 (1959); P. Eberhard, A. H. Rosenfeld, F. T. Solmitz, R. D. Tripp, and M. B. Watson, Phys. Rev. Letters 2, 312 (1959); A. H. Rosenfeld, Bull. Am. Phys. Soc. 3, 363 (1958).

[11] R. H. Dalitz and S. F. Tuan, Ann. Phys. (to be published).

[12] R. Karplus, L. Kerth, and T. Kycia, Phys. Rev. Letters 2, 510 (1959).

FIG. 7. The combined integrands of Eq. (14) for $\omega = 1.46$, $\omega_0 = 1.17$, and a smooth extrapolation of A_- into the unphysical region. The singularities of the integrand are indicated by vertical lines.

From the $\delta_0{}^-$-phase-shift combination, $d\sigma_+(1.46)/d\Omega|_{\theta=0}$ is 1.21 ± 0.16 mb/sr. If one assumes, as has been done here, that for lower K^+-meson energies $d\sigma_+{}^{el}(\omega)/d\Omega$ is isotropic, then $d\sigma_+{}^{el}(\omega)/d\Omega|_{\theta=0}$ simply becomes $\sigma_+{}^{el}(\omega)/4\pi$. Furthermore, $\sigma_+{}^{el}(\omega)=\sigma_+(\omega)$ for $\omega<1.46$. Thus, sufficient information is available for the determination of $D_+(\omega)$ for $\omega=1.0$, 1.17, 1.285, and 1.46.

The value of $D_-(\omega)$ is obtained from Eq. (15) in a similar way, but for $\omega=1.17$ and $\omega=1.285$. From bubble-chamber data, we have $d\sigma_-{}^{el}(1.17)/d\Omega|_{\theta=0}=5.2\pm1$ mb/sr.,[13] while $d\sigma_-{}^{el}(1.285)/d\Omega|_{\theta=0}$ is still not available. The total K^--p cross sections for the two energies are $\sigma_-(1.17)=91\pm9$ mb and $\sigma_-(1.285)=86\pm7$ mb. The value obtained for $D_-(1.17)$ is of the order of 0.5 K-meson Compton wavelength. For the higher energy, $D_-(1.285)$ is on the order of zero if $d\sigma_-{}^{el}(1.285)/d\Omega|_{\theta=0}$ is assumed to be not much larger than 8.2 mb/sr. This is not an unreasonable assumption, since $\sigma_-{}^{el}(1.285)=44\pm8$ mb. Thus D_- is small enough so that only a truly surprising change in the experimental data could change D_- enough to alter its effect in Eq. (14). The results of the calculations of $D_\pm(\omega)$ are listed in Table V.

TABLE V. $D_\pm(\omega)$ (the real part of the forward-scattering amplitude) for different ω's.

$D_\pm(\omega)$ $\diagdown$ ω	1.00	1.17	1.285	1.46
$D_+(\omega)$	-0.125 ± 0.14	-1.24 ± 0.14	-1.23 ± 0.14	-1.20 ± 0.08
$D_-(\omega)$	$\cdots$	±0.5	0	$\cdots$

The calculations have also been carried out[12] using the results of Dalitz[11] for D_- with no essential difference in the results.

Since it is clearly not possible to solve for $p_\Lambda g_\Lambda{}^2/4\pi$ and $p_\Sigma g_\Sigma{}^2/4\pi$ separately, we have assumed $p_\Lambda=p_\Sigma=p$ and $g_\Lambda{}^2=g_\Sigma{}^2=g^2$. By substituting the above experimental data into Eqs. (12) and (14), we can solve for $pg^2/4\pi$ for four different sets of values of ω and ω_0. The results are listed in Table VI. We see that for an attractive K^--p potential D_- is positive and a pseudoscalar coupling is favored; for a repulsive K^--p poten-

[13] R. D. Tripp, Lawrence Radiation Laboratory (private communication).

TABLE VI. Calculated values for the coupling constant for different combinations of ω and ω_0, for the possibility of either a scalar or pseudoscalar coupling. The term containing D_- has been included.

		$pg^2/4\pi$	
ω	ω_0	$p=+1$	$p=-1$
1.46	1.285	$(-0.20\pm0.68)-0.20D_-(1.285)$	$(-4.15\pm14)-4.2D_-(1.285)$
1.46	1.17	$(-0.09\pm0.38)-0.19D_-(1.17)$	$(-1.9\pm8)-4.0D_-(1.17)$
1.00	1.285	$(+0.09\pm0.38)-0.17D_-(1.285)$	$(+1.7\pm7)-3.2D_-(1.285)$
1.00	1.17	$(+0.25\pm0.58)-0.16D_-(1.17)$	$(+4.7\pm12)-3.4D_-(1.17)$

tial, D_- is negative and a scalar coupling is favored. If D_- is assumed to be negligible, the results from the first two rows favor a pseudoscalar coupling; those from the second two rows, a scalar coupling. The value of $g^2/4\pi$ varies about zero, but the variation is well within the statistical error. It is thus impossible to determine whether the coupling is scalar or pseudoscalar, but if it were scalar, $g^2/4\pi$ would be less than about 0.6; if pseudoscalar, less than about 10. These results indicate that even with the most recently available data it is difficult, from subtracted dispersion relations, to arrive at unambiguous conclusions as to the nature of the K-meson hyperon coupling.

ACKNOWLEDGMENTS